3ème Conférence Internationale sur les Sciences Appliquées et l'Innovation (CISAI-2025)
Proceedings Book Series –PBS- Vol 25, pp.9-15

Synthesis and characterization of spinel $ZnAl_2O_4$:SnO_2thin films for optoelectronic applications

Abdelmalek Kharroubi*[1], Hadj Benhebal[#2], Bedhiaf Benrabah[1],Touati Mohamed[1], Hireche Khaoula[1],Senni Amel[1]
[1]*Laboratory of Physical Engineering Faculty of Mater Sciences, University of Tiaret, Algeria*
[2]*Department of Chemical, Faculty of Mater Sciences, University of Tiaret, Algeria*
*[1]abdelmalek.kharroubi@univ-tiaret.dz

Abstract— **$ZnAl_2O_4$ and $ZnAl_2O_4$:SnO_2 thin films with(3%,6%)wt SnO_2 are deposited by the dip-coating technique on glass substrates and silicon substrates. Morphologic, optical and electrical properties of synthesized materials were investigated by atomic force microscopy (AFM). Fourier transform infrared spectroscopy, the ultra visible spectroscopy and complex impedance spectroscopy. The AFM images analysis revealed uniform surface and the effect of doping on the roughness of the layers has also been highlighted, we tracked the evolution of the surface roughness of the films as a function of the tin oxide content. The infrared transmission spectra obtained for different tin dioxide doping levels show a band observed at 655 cm^{-1} confirm the formation of the normal spinel structure, $ZnAl_2O_4$. The UV-Visible spectra show a high transmittance in the visible light range (T ~ 98% for pure $ZnAl_2O_4$ and between 85% and 86% for all doped samples). The optical gap varies from 3.80 eV (for the undoped) to 3.68 eV for the sample doped with 6% SnO_2. Complex impedance spectroscopy indicates that the effect of grain boundaries is dominant in the conduction mechanism. It is also observed that the equivalent circuit of undoped and SnO_2-doped $ZnAl_2O_4$ films is a parallel RC circuit.**
Keywords-**Sol-gel, $ZnAl_2O_4$, SnO_2-doped , Thin films**.

I. INTRODUCTION :

Metal oxides in thin films in general and $ZnAl_2O_4$ films in particular have potential applications in many fields, essentially when one simulates ousley needs good transparency in the visible and good electrical conductivity [1-3]. Zinc aluminate ($ZnAl_2O_4$) whose natural mineral called gahnite is a spinel oxide with cubic structure (space group Fd-3m) [1-2]. It has several advantages, such as high chemical and thermal stability, good catalytic activity, low-temperature sinter ability, and mechanical strength. In addition, it is classified as a transparent wide-bandgap semiconductor with estimated gap energy of 3.8 eV. Due to its characteristics, $ZnAl_2O_4$ is important in many technological applications such as catalysis, ceramics, aerospace, dielectrics, electronics, and optoelectronic devices [3-4]. It has been reported that the addition of metallic impurities, in the form of atoms or oxides to $ZnAl_2O_4$ adjusts both the crystallite size and the bandgap, resulting in an improvement in many properties and consequently offering greater application potential [5-7]. In this work, sol-gel process was chosen to produce the $ZnAl_2O_4$ films. It makes it possible to obtain a material of high purity having good homogeneity compared to other conventional production methods such as chemical vapor deposition, pyrolysis or spraying. X-ray powder diffractograms of pure Gahnite.

II. EXPERIMENTAL

A. Samples synthesis

Zinc nitrate hexahydrate $Zn(NO_3)_2.4H_2O$, Aliminium nitrate $Al(NO_3)_2.3H_20$, ethanol (C_2H_5OH), oxalic acid $C_2H_2O_4$ were used to prepare pure and SnO_2-doped $ZnAl_2O_4$ thin films prepared by sol-gel method and deposited on properly cleaned Pyrex substrates ($75\times 25\times 1\ mm^3$) using a dip-coaing with a withdrawal speed of 50 mm/min. The formed films pass through the drying step in order to evaporate the solvent, finishing all that with a heat-treatment when the films were annealed in muffle furnace at 500°C for 15 min.

B. Samples characterization

ISSN: 2961-6611

3ème Conférence Internationale sur les Sciences Appliquées et l'Innovation (CISAI-2025)
Proceedings Book Series –PBS- Vol 25, pp.9-15

The Morphology characterization of the film was analysed using a JEOL JSPM-5200.The optical properties were determined by optical transmittance measurements of the films using UV-1650 Shimadzu spectrophotometer in the wavelength range from 300 to 900 nm. FTIR spectra of the samples were recorded using a Shimadzu 8400 Spectrometer in the wave number range from 400 cm^{-1} to 4000 cm^{-1}. The electrical characteristics were highlighted by impedance measurements performed using an Agilent 4284A LCR meter operating in the frequency range 75 kHz to 20 MHz with oscillation amplitude of 1 V.

III. SAMPLES CHARACTERIZATION

A. AFM analysis

Figure 1 shows 5 µm × 5 µm AFM images obtained for the pure and SnO_2 doped $ZnAl_2O_4$ films deposited onto glass substrates. Although each film exhibits a homogeneous distribution of grains, there is a visible change in the morphology of the films when they were doped tin oxyde. This is due to the coalescence of grains resulting at the effect of SnO_2 on the $ZnAl_2O_4$ matrix [8-10].

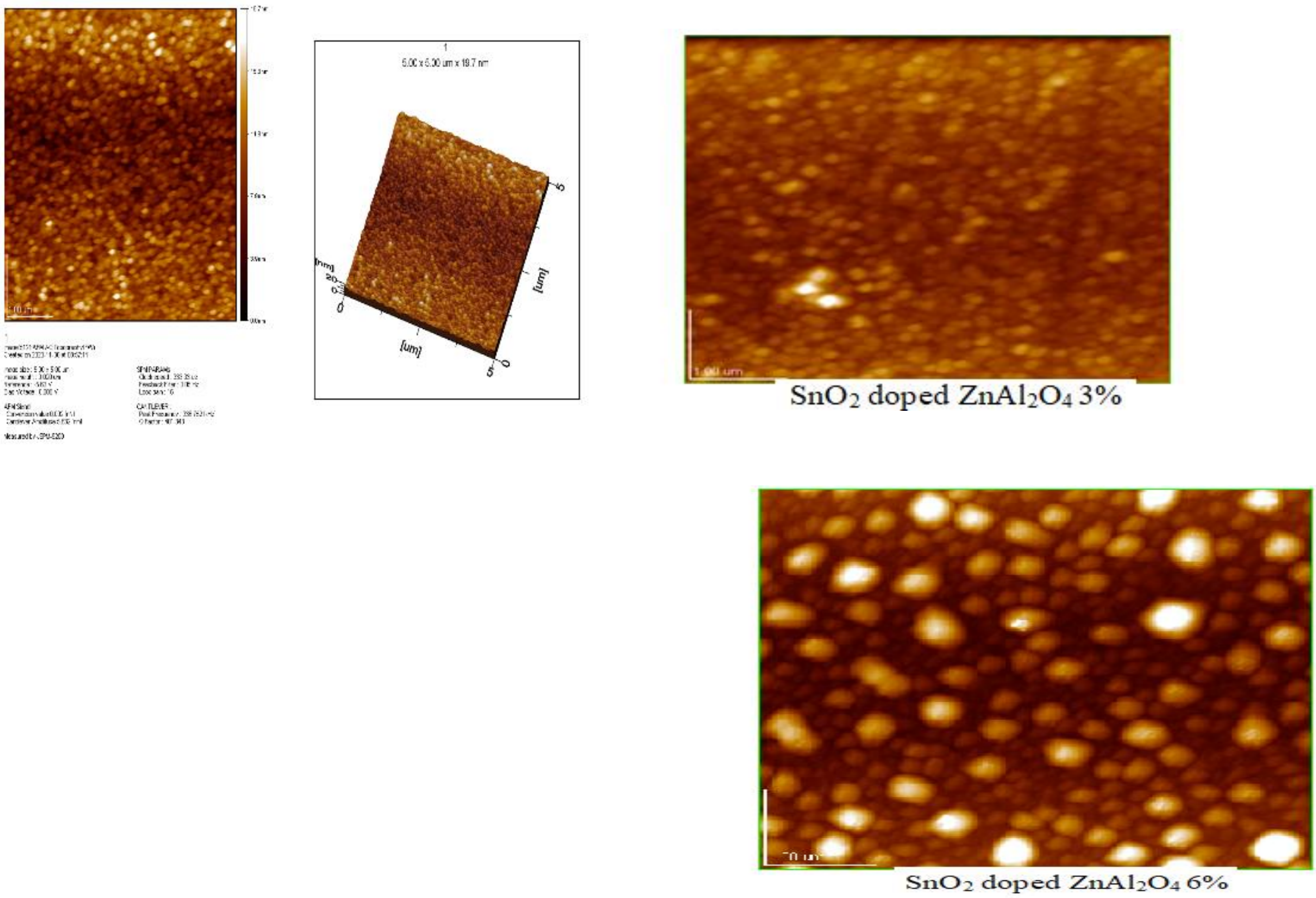

Fig.3 AFM images of pure SnO2 doped ZnAl2O4 thin film

B. FTIR Analysis

ISSN: 2961-6611

FTIR spectra were measured in the wavenumber region 400-4000 cm^{-1}. The band recorded at 3599 cm^{-1} can be attributed to the stretching vibration of H_2O molecules [11]. The small peak observed at 1444 cm^{-1} can be attributed to Al-O stretching vibrations [12].

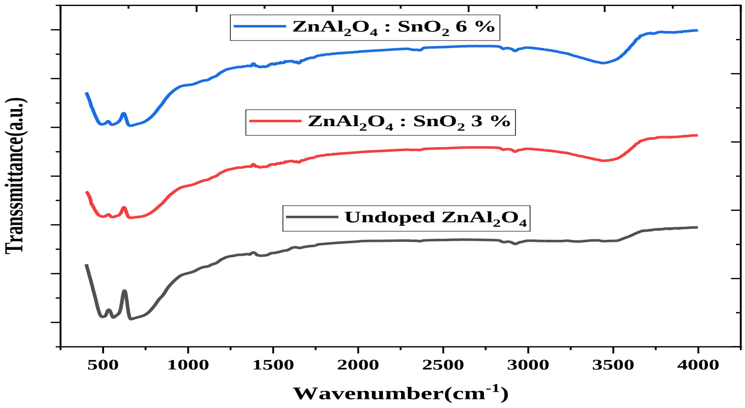

Fig. 2. FTIR spectra of pure and SnO_2-doped $ZnAl_2O_4$ thin Films

The bands at 655 cm^{-1} confirm the formation of the normal spinel structure, $ZnAl_2O_4$. These spinel peaks at 655 cm^{-1} are consistent with those observed by Abdullah et al. The bands observed in the low-frequency region of the spectrum 487-550 cm^{-1} correspond to the different structures that may form, including zinc oxide and various aluminum oxides [13].

C. .UV–Visible spectroscopy:

Fig. 3 shows transmission spectra of the pure $ZnAl_2O_4$ and SnO_2 doped $ZnAl_2O_4$ films. The transmission spectra have a general shape characterized by the presence of two distinct regions. We note that the films have a good transparency in the visible 80-95%, which varies slightly with tin oxide doping.

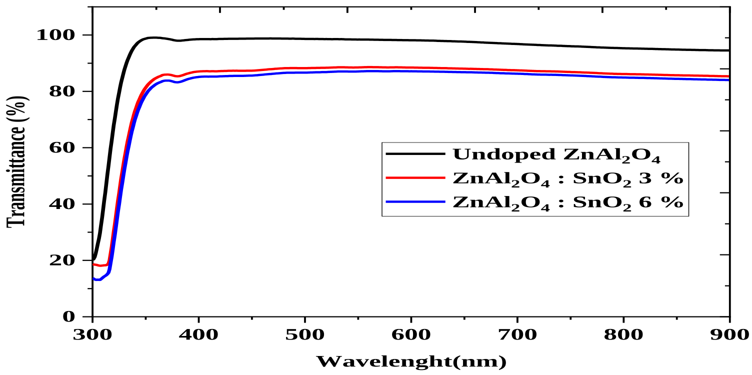

Fig.3. Transmittance spectra of pure and SnO_2-doped $ZnAl_2O_4$ films.

By exploiting the Tauc relationship of equation (4), the optical band gap of undoped $ZnAl_2O_4$ and SnO_2-doped (3 and 6%) thin films (Table 2) was determined [14].

$$(\alpha h\nu)^{\frac{1}{n}} = A[h\nu - Eg] \ldots\ldots (2)$$

ISSN: 2961-6611

Where 'a' indicates the absorption coefficient, 'A' is a constant; 'h' corresponds to photon energy and 'Eg' stands for the optical band gap of the material. The value of n corresponds to 1/2 and 2 are for direct and indirect band gap transitions respectively.

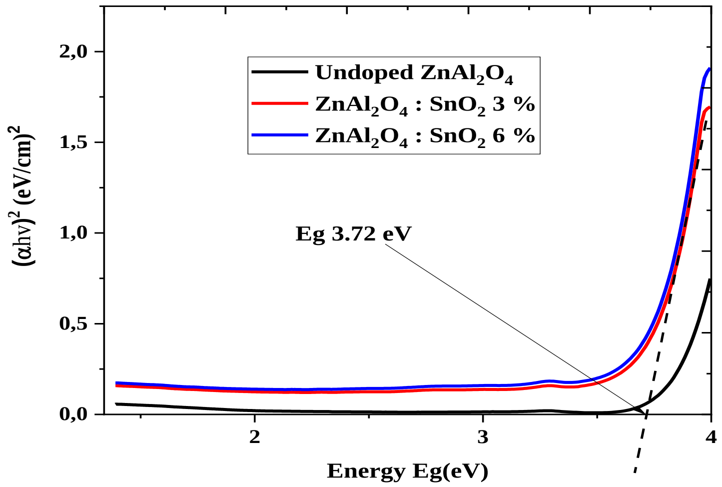

Fig.4. Tauc plot of pure and SnO_2-doped $ZnAl_2O_4$

Samples	Eg (eV)	Refractive index(n)
Pure $ZnAl_2O_4$	3.80	2.224
$ZnAl_2O_4$: SnO_2 3%	3.72	2.236
$ZnAl_2O_4$: SnO_2 6%	3.68	2.241

Table 2. Band gap values and refractive index of SnO_2 doped and undoped $ZnAl_2O_4$

Furthermore, the absorption intensity of the doped samples in the ultraviolet region increased significantly, and the absorption edge shifted towards longer wavelengths with increasing SnO_2 concentration [15]. This could be due to the interaction between Sn^+ ions with the $ZnAl_2O_4$ matrix, which contributed to the excitation of the generated carriers [16].

D. Complex impedance spectroscopy

Figure 5 is the Nyquist representation of $ZnAl_2O_4$ thin layers with undoped and SnO_2 doped , where the frequency varies from 75kHz to 1MHz at ambient temperature.

ISSN: 2961-6611

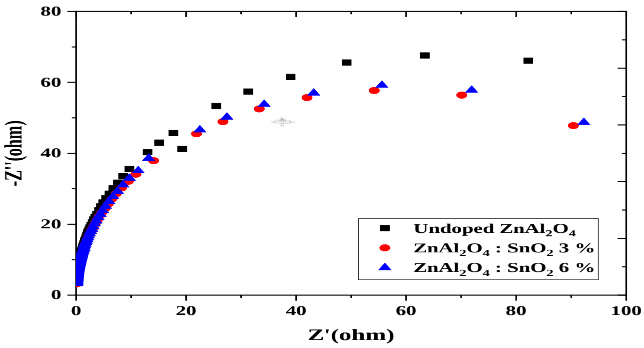

Fig.5 Nyquist plots of pure and SnO_2 doped and undoped $ZnAl_2O_4$

Samples	**f_{max}(KHZ)**	**R_p (Ω)**	**C (nF)**
Pure $ZnAl_2O_4$	519.45	67.74	3.06
$ZnAl_2O_4$: SnO_2 3%	519.44	57.7	5.31
$ZnAl_2O_4$: SnO_2 6%	519.46	59.2	5.18

Table 3. Values of fc, Rp and C of undoped and SnO2-doped ZnAl2O4 films

From Table 3 , it can be seen that the resistance Rp decreases while increasing the doping level of SnO_2, reaching a value of 59.2 Ω for a doping level of 6%, while the capacitance increases from 3.06 nF to 5.18 nF for the same doping of 6% in SnO_2.The variation in this capacitance is related to the formation of oxygen vacancies, which is likely due to the substitution of Zn^{2+} by Sn^{3+} or Sn^{+} ions at the grain surfaces [17].

IV. CONCLUSION

In this work, we prepared by the sol-gel process thin films of undoped $ZnAl_2O_4$ and doped 3%, 6%with SnO_2. The AFM images analysis showed that the surface roughness of the SnO_2 doped $ZnAl_2O_4$ had rougher surface compared with other samples. The particle size decreases with the increase of SnO_2 content in the prepared samples.FTIR spectra showed the presence of peaks related to bond vibrations in the spinel structure, thus confirming the formation of the materials.The UV-Visible spectroscopy, the transmission rate in the visible range varies from between 90% for thin films 1layer and 95%. The optical band gap was reduced from 3.80 to 3.68 eV upon doping due to the polarization induced by the increase in charge caused by the introduction of impurities.The impedance measurements show that the equivalent circuit of the diagram of $ZnAl_2O_4$ films is an RpCp parallel when the resistance Rp decreases while the capacitance Cp increases with SnO_2 doping.Based on these results, we conclude that SnO_2 doping allows obtaining $ZnAl_2O_4$ thin films with very interesting structural and optical properties, making these films a good alternative for optoelectronic applications, such as LEDs and lasers.

REFERENCES

[1] YANG, Lan, ZHAO, Yajie, YIN, Rui, et al. Synthesis of Ni 2+-doped $ZnAl_2O_4$/ZnO Composite Phosphor Film with Largely Enhanced Polychromatic Emission via a Single-Source Precursor. *Journal of the American Ceramic Society*, 2014, vol. 97, no 4, p. 1123-1130.

ISSN: 2961-6611

[2] MOHAMED, Salah , *et al.* Novel antimicrobial biodegradable composite films as packaging materials based on shellac/chitosan, and $ZnAl_2O_4$ or $CuAl_2O_4$ spinel nanoparticles. *Scientific Reports*, 2024, vol. 14, no 1, p. 27824.
[3] JALAL, Wan Nasarudin Wan, ABDULLAH *al.* Characteristics of nanostructured CaxZn (1-X) Al_2O_4 thin films prepared by sol-gel method for GPS patch antennas. *Sains Malaysiana*, 2014, vol. 43, no 6, p. 833-842.
[4] GURUGUBELLI, Thirumala Rao, BABU, Bathula, et YOO, Structural, optical, and magnetic properties of cobalt-doped $ZnAl_2O_4$ nanosheets prepared by hydrothermal synthesis. *Energies*, 2021, vol. 14, no 10, p. 2869.
[5] SIRAGAM, Srilali, DUBEY, Raghvendra Sarvjeet, PAPPULA, Lakshman, *et al.* Zinc aluminate-based composite nanoparticles for microwave applications. *ACS omega*, 2022, vol. 7, no 27, p. 23393-23400.
[6] MARTINS, Renata F. et SERRA, Osvaldo A. Thin film of $ZnAl_2O_4$: Eu^{3+} synthesized by a non-alkoxide precursor sol-gel method. *Journal of the Brazilian Chemical Society*, 2010, vol. 21, p. 1395-1398.
[7] SADEK, H. E. H., REDA, A. E., KHATTAB, R. M., *et al.* The Role of TiO_2 on $ZnAl_2O_4$ Spinel Prepared by Direct Coagulation Casting Method: Physico-mechanical, Optical, Structural and Antimicrobial Properties. *Journal of Inorganic and Organometallic Polymers and Materials*, 2024, vol. 34, no 3, p. 1350-1368.
[8] BATTISTON, Suellen, RIGO, Caroline, SEVERO, Eric da Cruz, et al. Synthesis of zinc aluminate (ZnAl2O4) spinel and its application as photocatalyst. Materials research, 2014, vol. 17, p. 734-738.
[9] DU, Xuelian, LI, Liqiang, ZHANG, Wenxing, et al. Morphology and structure features of ZnAl2O4 spinel nanoparticles prepared by matrix-isolation-assisted calcination. Materials Research Bulletin, 2015, vol. 61, p. 64-69.
[10]ZULFAKAR, Mohd Syafiq, ABDULLAH, Huda, ISLAM, Mohammad Tariqul, et al. Performance effect of ZnAl2O4-SiO2 thin film for wireless patch antenna application. Journal of Nano Research, 2014, vol. 28, p. 141-150.
[11] HUANG, Shangpan, WEI, Zhiqiang, WU, Xiaojuan, et al. Optical properties and theoretical study of Mn doped ZnAl2O4 nanoparticles with spinel structure. Journal of Alloys and Compounds, 2020, vol. 825, p. 154004.
[12] DE SOUZA, Luiz KC, ZAMIAN, José R., DA ROCHA F, *et al.* Blue pigments based on CoxZn1− xAl2O4 spinels synthesized by the polymeric precursor method. *Dyes and Pigments*, 2009, vol. 81, no 3, p. 187-192.
[13] ABDULLAH, Huda, WA, *et al.* Fabrication and Characterization of TiO_2-Doped $ZnAl_2O_4$ Nanocrystals via Sol-Gel Method for GPS Antenna. In : *Materials Science Forum*. Trans Tech Publications Ltd, 2016. p. 331-344.
[14] TIAN, Qingwen, RAN, Miao *et al.* $ZnAl_2O_4$/$BiPO_4$ composites as a heterogeneous catalyst for photo-Fenton treatment of textile and pulping wastewater. *Separation and Purification Technology*, 2020, vol. 239, p. 116574.
[15] MOTLOUNG, S. V., *et al.* Effects of Cr3+ mol% on the structure and optical properties of the $ZnAl_2O_4$: Cr^{3+} nanocrystals synthesized using sol–gel process. *Ceramics International*, 2015, vol. 41, no 5, p. 6776-6783.
[16] MOTLOUNG, S. V., DEJENE, F. B., KOAO, L. F. *et al.* Structural and optical studies of ZnAl2O4: x% C^{2+} ($0< x\leq 1.25$) nanophosphors synthesized via citrate sol-gel route. *optical materials*, 2017, vol. 64, p. 26-32.
[17] B. Chen, J. Sha, X. Ye, Z. Jiao, et L. Zhang, « Dielectrical behavior of nanostructured α-Fe_2O_3 with different annealed temperatures », Sci. China Ser. Math., vol. 42, no5, p. 510, mai 1999.

ISSN: 2961-6611